A Sensor Based on Nanoantennas

Ricardo Alexandre Marques Lameirinhas
ricardo.lameirinhas@tecnico.ulisboa.pt

Instituto Superior Técnico, Universidade de Lisboa, Lisboa, Portugal

***Abstract*—At the end of the XX century a new phenomenon was discovered by Ebbesen, the extraordinary optical transmission. He reported that metallic arrays composed by nano holes - also called nanoantennas -, can support resonant optical transmissions responsible to amplify and concentrate electromagnetic radiation. This is an extraordinary phenomenon, because classical diffraction theories can not predict it. This article shows the timeline of theories that try to model the interaction between light and metal planes with slits, holes, grooves or apertures. The comparison between theories is done. Furthermore, as the optical response of these nanoantennas is dependent on the complex dielectric function, there is a high probability of successfully use these structures as sensors. This article aims to verify how the structure parameters - periodicity, hole diameter, nanoantenna thickness and substrate thickness -, can influence the optical response in order to tune the spectrum. Using *COMSOL Multiphysics*, several 3D simulations aim to conclude about the parameters influence on an air-gold-quartz and an air-aluminium-quartz structures, being the nanoantenna made with gold and aluminium. Moreover, all the simulations allow us to verify high amplified areas near the metal surface and a resonant spectral response. This is a clear evidence of a energy exchange due to the generation and propagation of surface plasmon polaritons. Based on the spectra taken from the parameter analysis, it was chosen an specific structure to test two different sensors. A temperature sensor and a tissues detection sensor were tested and the simulations are presented. It is concluded that a nanostructure based on a nanoantenna can be used as a sensor for several applications.**

***Index Terms*—Nanoantennas; Optoelectronic devices; Sensors; Subwavelength structures; Surface plasmons polaritons.**

I. Introduction

The interaction between electromagnetic waves - for instance, light -, and matter was always a topic that aroused interest to the scientific community [1], [2]. Mainly because some phenomena were discovered recently, as the extraordinary optical transmission - EOT -, and based on them it has been possible to develop new devices [3], [4].

The resonant behaviour characteristic from EOT is affected by the complex dielectric function, which also depends on the incident wavelength. The complex dielectric function is often presented as a fitting of the Drude-Lorentz model, for each material [5], [6].

The variation of the complex dielectric function with physical or chemical events can be useful to develop a sensor. This kind of sensors can be designed for many application in different fields such as medicine, chemistry, defence, communications, energy or environment [4].

A nanoantenna - which is a subwavelength hole structure that supports EOT -, can be tuned and its material can be chosen in order to fulfil spectral specifications - for example, gain, bandwidth or peak position -. Thus, it is possible to design the sensor optical response [7]–[18].

It is expected that this new kind of sensors, in the near future, will be classified as standalone, miniaturised, portable and they will have high sensibilities and huge detection limits [15]–[18]. However, the improvement of computational methods and of new techniques of manufacturing are leading the process of creating new nanotechnological devices. Thus, sensors based on nanoantennas are not exceptions and they are quite important factors to decrease the fabrication costs and increase the reproducibility and the probability to commercialise these devices [4], [15]–[18]. Even that, it is needed to find models to be able to clarify how the spectrum changes regarding the parameters tuning [19]–[25]. This article not only aims to analyse the parameter influence, but also presents simulations from two different sensors applications.

II. Evolution of the Theoretical Foundations

Since the XVII century, experiments and theories have been proposed as explanations and models for the light behaviour and interactions with matter [1], [2]. In this century, Huygens stated that each unobstructed point from a plane wave front can be analysed as a punctual source, emitting a spherical wave with the same characteristics from the main - real -, wave [1], [2]. However, only on the XVIII century, Fresnel reformulated the Huygens principle in order to consider curve waves. This was a huge progress, because it aims on the study of the near-field regime. To assume a plane wave, the distance between the source and the target - where the analysis is performed -, should be very large and, in this condition, geometrical optics methods can aim to analyse the wave propagation [1], [2].

On the begging of the XIX century, Young proved the wave characteristic of light, using a double slit experiments and the Huygens-Fresnel principle [1], [2].

Fraunhofer also used the Huygens principle to compose his diffraction theory, that relates the irradiance at a certain angle of diffraction θ and the main lobe one - $\theta = 0^\circ$ -, after the wave propagates though a slit in a metallic plane. Nonetheless, as presented on expression 1, for N slits, the relation is between the irradiance at a certain angle and an irradiance I_0, that is the contribution of each equal slit for the overall irradiance [1], [2], [4]. However, he assumed a plane and monochromatic wave, characterised by an incident wavelength λ and a wavevector

$\bar{\boldsymbol{k}}$, with perpendicular incidence to a perfect conductive metal, where are N slits of a diameter and they are spaced by a distance of d [1], [2], [4]. The analysis target is over the slits plane, at a distance D and the distance between the plane position given by θ and the main lobe one is given by y [1], [2], [4]. Fraunhofer determine the maximum and the minimum intensity positions, y, on the target, regarding the constructive and destructive interference among different rays propagating from the slits plane [1], [2], [4]. Expressions 2 and 3 are obtained using these distance definitions and under the far-field assumption - $D \gg y$ -, [1], [2], [4].

$$I(\theta) = I_0 \left(\frac{sin(\beta)}{\beta}\right)^2 \left(\frac{sin(N\alpha)}{\alpha}\right)^2 \tag{1}$$

$$\beta = \frac{ka}{2} sin(\theta) = \frac{\pi a}{\lambda} sin(\theta) = \frac{\pi a y}{\lambda D} \tag{2}$$

$$\alpha = \frac{kd}{2} sin(\theta) = \frac{\pi d}{\lambda} sin(\theta) = \frac{\pi d y}{\lambda D} \tag{3}$$

After that, Kirchhoff composed his theory, that includes as limit cases the Fresnel and Fraunhofer's theories [4], [26]. He assumed the propagation of a plane and scalar wave along x direction and an opaque plane perpendicular to it [4], [26]. The opaque plane has an aperture and the transmitted wave propagation is determined by expression 4, that degenerates on expression 5, using Green's theorem [26]. The scalar wave is $\bar{u}$ and the integration coordinates should be y' and z', such as x', y' and z' are the coordinates of a point $\boldsymbol{r'}$ before or over the metal surface. Moreover, $\boldsymbol{\phi}$ is the Green's function, for a monochromatic wave at a point $\boldsymbol{r}$ after the plane, given by $r^2 = x^2 + y^2 + z^2$.

$$\nabla^2 \bar{u} + k_0^2 \bar{u} = 0 \tag{4}$$

$$u(\boldsymbol{r}) = \frac{1}{4\pi} \int \left[-\frac{\partial u}{\partial x'}(\boldsymbol{r'})\, \boldsymbol{\phi}(|\boldsymbol{r} - \boldsymbol{r'}|) + u(\boldsymbol{r'}) \frac{\partial \boldsymbol{\phi}}{\partial x'} \right] d\sigma \tag{5}$$

However, boundary conditions are not verified at the metal surface on Kirchhoff's theory, since he assumed an opaque and finite plane [4], [26]. As the incident and reflected waves do not exist over the surface, these conditions are not satisfied, specially on the surfaces near the slits [26]. For subwavelength structures and for the near-field regime, this problem can not be neglected. Thus, in 1944, Bethe presented his theory, assuming an infinite and perfect conductive metal plane with a circular hole [4], [26]. Bethe's goal was to improve Kirchhoff's theory, fulfilling the boundary conditions. However, years later, Bouwkamp showed that Bethe's equations do not verify it and he amend it, using the Babinet's principle [4], [27]. Expressions 6 and 7 are the Bouwkamp's results from the electric and the magnetic vectors, when the wave propagation is on the z direction [4], [27]. Nonetheless, Bethe showed - and Bouwkamp reformulated the expressions, but he took the same conclusions -, that hole structures can behave as an electric and a magnetic dipole and, using Poynting's theorem, it is possible to determine the complex radiation power. When applying the subwavelength hole condition to this expression, it results show that the radiation power decay should be proportional to λ^{-4} [4], [26], [27].

$$\bar{\boldsymbol{E}}(\boldsymbol{r}) \Rightarrow \begin{cases} \bar{E}_x = -\dfrac{4ik}{3\pi} \dfrac{2a^2 - x^2 - 2y^2}{\sqrt{a^2 - x^2 - y^2}} \\ \bar{E}_y = -\dfrac{4ik}{3\pi} \dfrac{xy}{\sqrt{a^2 - x^2 - y^2}} \\ \bar{E}_z = 0 \end{cases} \tag{6}$$

$$\bar{\boldsymbol{H}}(\boldsymbol{r}) \Rightarrow \begin{cases} \bar{H}_x = 0 \\ \bar{H}_y = \dfrac{1}{\mu_0 c} \\ \bar{H}_z = -\dfrac{4}{\mu_0 c \pi} \dfrac{y}{\sqrt{a^2 - x^2 - y^2}} \end{cases} \tag{7}$$

III. Surface Plasmons Polaritons and The Extraordinary Optical Transmission

In 1998, Ebbesen reported that nanostructures, composed by periodic circular holes, can amplify and concentrate electromagnetic radiation [3]. These structures, also known as nanoantennas, allow an unexpected transmission spectrum. This phenomenon was called extraordinary optical transmission and Ebbesen stated that its main agents are the surface plasmons polaritons [3]. This phenomenon can not be predicted by the classical theories, since it is possible to amplify light using nano holes and because classical theories only allow to verify intensity decays. Two conditions are fundamental to the excitation of this polaritons, considering that the metal has a complex dielectric function given by $\bar{\epsilon_1} = \epsilon_1' + j\epsilon_1''$ and the dielectric medium is characterised by a real function ϵ_2: (i) $\epsilon_1' < 0$ and $|\epsilon_1'| > \epsilon_2$; (ii) A match between the wavevector of the polariton and the parallel component one of the incident light with the interface [4], [28]–[31].

Years later, Lalanne e Hugonin did an analytical study from the Maxwell's equations, that proved the propagation of surface plasmons polaritons, as a fundamental stage for this phenomenon, as well as its combination with a creeping wave propagation [31].

In the 1950's the interest in plasmons receive a great impulse with the works of Pines and Bohm. Later, in 1956 Fano introduces the concept of polariton and in 1957 Ritchie presented the first theoretical description of surface plasmons. Surface plasmons polaritons TM propagation equations are presented on expression 8, for a surface at $z = 0$, where there is metal/plasma for $z < 0$ and dielectric for $z > 0$ [4], [28]–[30]. Thus, the plane is extended along y axis and there are oscillations along x and an exponential decay over z direction.

A plasmon is the redistribution of the plasma's free electrons - a quantum of a plasma oscillation -, [4], [28]–[31]. Light is also an oscillation of particles, in this case the photons. Both oscillations can couple and in this case the polariton is created. A polariton, a quasiparticle as the plasmon is, is the result of a strong coupling between an electromagnetic wave - light in this case -, and an electric or magnetic dipole - the nanoantenna as verified on Bethe's and Bouwkamp's theories -, [4], [26]–[30]. This energy exchange is a resonant behaviour, capable

to amplify and concentrate electromagnetic energy near the surfaces.

$$\begin{cases} \bar{E}_{x,m}(x,y,z,t) = E_0 e^{j(\bar{k}_x x + \bar{k}_{z,m}|z| - \omega t)} \\ \bar{E}_{z,m}(x,y,z,t) = \pm \dfrac{\bar{k}_x}{\bar{k}_{z,m}} E_0 e^{j(\bar{k}_x x + \bar{k}_{z,m}|z| - \omega t)} \\ \bar{H}_{y,m}(x,y,z,t) = H_0 e^{j(\bar{k}_x x + \bar{k}_{z,m}|z| - \omega t)} \end{cases} \quad (8)$$

When extraordinary optical transmission was discovered by Ebbesen, he sooner reported that this resonant behaviour can be useful to develop a new type of miniaturised photonic devices, as optical sensors [3].

IV. Structure Parameters Evaluation

This article will show the resonant behaviour of the EOT, as well as the capability of amplify and concentrate electromagnetic radiation, proving that it is possible to design a optical sensor using its resonant properties. The first step to develop a structure is to try to understand how its parameters can influence the output spectrum.

Several simulations were performed in order to verify the variation of the spectral response regarding parameter sweeps - periodicity, hole diameter, nanoantenna thickness and substrate thickness -, [7], [9], [10], [12], [16], [20]. These sweeps are done based on a reference structure, presented on figure 1. It is a 3x3 squared array structure, composed by circular holes and characterised by a periodicity of $a_0 = 0.5\,\mu\text{m}$, a hole diameter of $d = 150\,\text{nm}$, a nanoantenna thickness of $t = 100\,\text{nm}$, as well as a substrate thickness of $t_{sub} = 50\,\text{nm}$. Also, the dielectric medium has a thickness of $200\,\text{nm}$ however, it is measured from the interface between the nanoantenna and the substrate in order to set the hole medium as dielectric.

An electric field, defined by a norm of $|E_0| = 1\,\mu\text{V}\,\text{m}^{-1}$, is generated on the top of the structure presented on figure 1 - that is on the external boundary of the dielectric medium -, and it is perpendicular incident on the nanoantenna, having the z axis opposite direction. Thus, on the generation port, this electric field was defined as $|E_x| = |E_y| = \frac{1}{\sqrt{2}}\,\mu\text{V}\,\text{m}^{-1}$ and $|E_z| = 0\,\mu\text{V}\,\text{m}^{-1}$. Furthermore, all the external boundaries are total absorbent, meaning that there is no reflection.

Moreover, all the simulations are done for 250 equidistant wavelength points, from $250\,\text{nm}$ to $1200\,\text{nm}$. The frequency analysis is done using a boundary probe - on/under the substrate - and measuring the square of the maximum ratio between the electric field norm and the incident electric field norm, $|\frac{E}{E_0}|^2$.

All the spectra that will be presented are only possible to reach due to the generation and propagation of surface plasmons polaritons, near the interfaces, as it is possible visualise on figure 2. On this figure, it is quite noticeable that in these regions, there are field amplification, because the electric field norm is higher than the incident one.

In this article, it is analysed a structure composed by an air dielectric medium and a quartz substrate. The optical response of a gold and an aluminium nanoantenna is going to be shown.

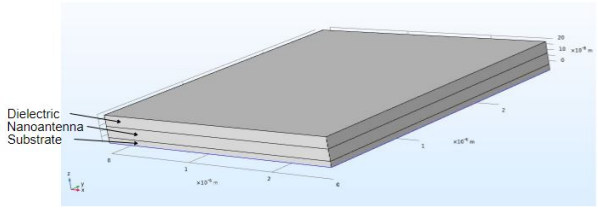

Fig. 1. Topology of the simulated structure.

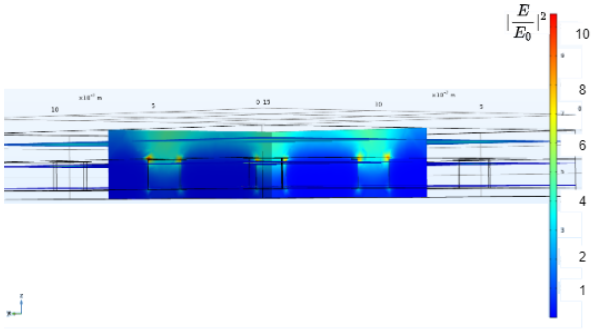

Fig. 2. Observation of the generation and propagation of surface plasmon polaritons.

The complex dielectric function can related to the complex refractive index function by $\bar{\epsilon} = \epsilon' + j\epsilon'' = \bar{n}^2 = (n + jk)^2$ such as $\epsilon' = n^2 - k^2$ and $\epsilon'' = 2nk$. On the other hand, $\epsilon''(\omega) = \frac{\sigma(\omega)}{\epsilon_0 \omega}$, where the conductivity of the material is given by $\sigma(\omega)$, and so that it is possible to relate Ohmic losses with ϵ''. Furthermore, dispersion losses are related to the real part of the complex refractive index, n, and so that, materials can be chosen analysing its optical properties and the functions values for its frequency/wavelength.

Air, modelled by the Ciddor's results, is chosen as the dielectric medium, because it is the most common dielectric medium and it is easy to characterise, allowing a wider range of application areas, without being too restrictive [32].

Gold, modelled by the Rakic's Drude-Lorentz fitting, has its transition between Drude and interband regimes at approximately $2\,eV \sim 2.3\,eV$, *i.e.*, $530\,\text{nm} \sim 600\,\text{nm}$, being used on the red and near-infrared regions [11], [12], [32]. Using aluminium is possible to obtain gain along all visible region. Aluminium has a larger negative real part of its dielectric function, and it is used for wavelengths between $400\,\text{nm}$ and $650\,\text{nm}$. It is the result of an almost null dielectric function imaginary part until $500\,\text{nm}$. After it, its value is going to increase until a maximum located around $800\,\text{nm}$, making this material of the worst to be used on the red and near-infrared region applications and the best one to create gain along all the visible region.

Although the optical properties can allow us to select a metal in alternative to others, it is also important to analyse the chemical stability of these metals, in order to know if the material will keep the same or if their chemical formula will change along time, leading to adjustments on their own optical properties and consequently, to the output spectrum. In this

aspect, some passivation layers will be formed on aluminium, resulting in Al_2O_3, whereas gold is known to have an excellent stability [11], [12], [32].

It is chose quartz - SiO_2 -, as the substrate, modelled by, Gao's results, because it will not have a huge influence on the output spectrum, since its transition between Drude and interband regime is around $0.15\,eV$ - $8000\,\mathrm{nm}$ -, [32]. Quartz complex dielectric function has null imaginary part along all the simulated range, as well as a real part with small variations. Thus, the inclusion of this substrate will not create a new resonant peak in the simulated range. Furthermore, it is a hard material that allows high temperatures, suitable to guarantee some protection and robustness to the structure.

A. Periodicity Sweep

First, it is performed the periodicity sweep for $a_0 = 0.3\,\mu\mathrm{m}$, $a_0 = 0.5\,\mu\mathrm{m}$, $a_0 = 0.7\,\mu\mathrm{m}$ and $a_0 = 0.9\,\mu\mathrm{m}$, as presented on figures 3 and 4, respectively for the gold and the aluminium nanoantenna. On the gold, it is obvious that when the periodicity increases, the peak intensity diminish and the peak wavelength keeps around the same value. However, this rule can not be verified for every material, which is the case of aluminium.

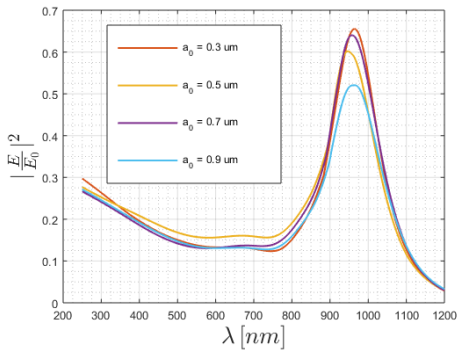

Fig. 3. Periodicity sweep on a gold nanostructure with a quartz substrate.

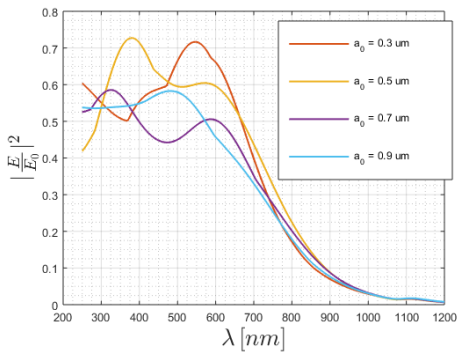

Fig. 4. Periodicity sweep on an aluminium nanostructure with a quartz substrate.

B. Hole Diameter Sweep

After that, the hole diameter was swept from $d = 50\,\mathrm{nm}$ until $d = 200\,\mathrm{nm}$, using a $50\,\mathrm{nm}$ step. Gold and aluminium responses are respectively presented on figures 5 and 6.

In both cases, it is visible that the higher the diameter is, the stronger the field intensity is. Nevertheless, it is important to mention that the subwavelength hole diameter condition should not be neglected in order to have the resonant behaviour that is characteristic of the EOT phenomenon. Moreover, on the gold spectra this parameter can be used to shift the output spectrum within a certain wavelength range. On the aluminium structure the gain region expands however, more to the red-side than to the blue-side.

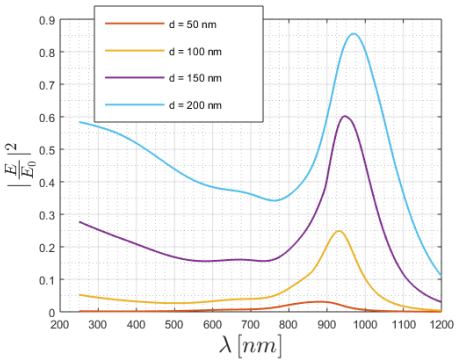

Fig. 5. Hole diameter sweep on a gold nanostructure with a quartz substrate.

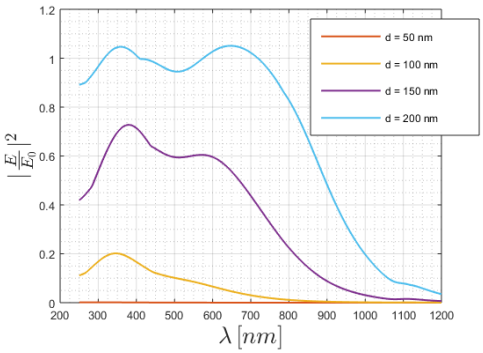

Fig. 6. Hole diameter sweep on an aluminium nanostructure with a quartz substrate.

C. Nanoantenna Thickness Sweep

The nanoantenna thickness sweep results are respectively presented on figures 7 and 8, for the gold and the aluminium nanoantenna. Here, it is very important to refer again that the nanoantenna is inside the dielectric medium. This one has a thickness of $200\,\mathrm{nm}$ and so that, when the nanoantenna thickness is varying, it is also varying the air medium thickness. This is an important statement, because all the conclusion that can be taken will continue to be based on the assumption that the distance between the port - where the electromagnetic

wave is generated -, and the nanoantenna rear - which is in contact with the substrate - remains constant.

Analysing the values for $t = 50\,\text{nm}$, $t = 100\,\text{nm}$ and $t = 150\,\text{nm}$ it is possible to conclude that the thicker the nanoantenna is, the lower intensity values. In addition to it, the aluminium response seems to be flatter as the nanoantenna becomes thicker.

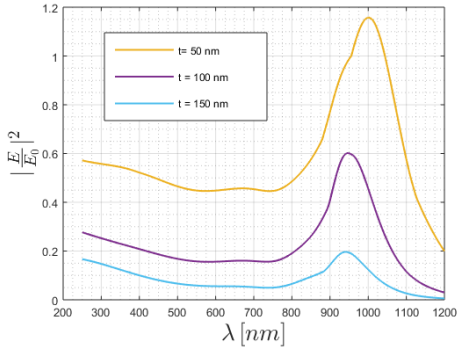

Fig. 7. Nanoantenna thickness sweep on a gold nanostructure with a quartz substrate.

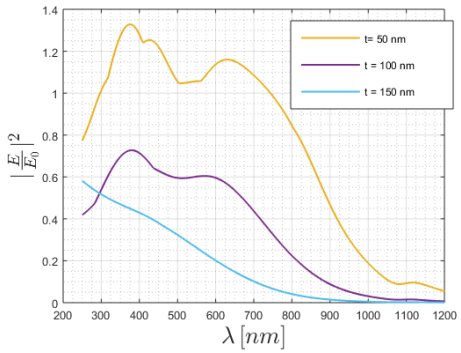

Fig. 8. Nanoantenna thickness sweep on an aluminium nanostructure with a quartz substrate.

D. Substrate Thickness Sweep

The last sweep analysed in this article is the substrate thickness. It is expected that as the substrate becomes thicker, the dispersion losses will be higher and, consequently, the field intensity will diminish. Based on figures 9 and 10 it is possible to verify it, respectively for the gold and aluminium structures. However, if the substrate becomes too thin, the generation and propagation of the surface plasmons polaritons is compromised and, consequently, the electric field is going to be weaker than expected, as verified on figure 9, where the gold response for $t_{sub} = 20\,\text{nm}$ reveals a smaller intensity peak in comparison with its response for $t_{sub} = 30\,\text{nm}$ and $t_{sub} = 40\,\text{nm}$.

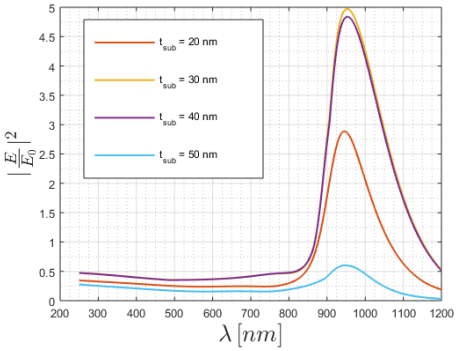

Fig. 9. Substrate thickness sweep on a gold nanostructure with a quartz substrate.

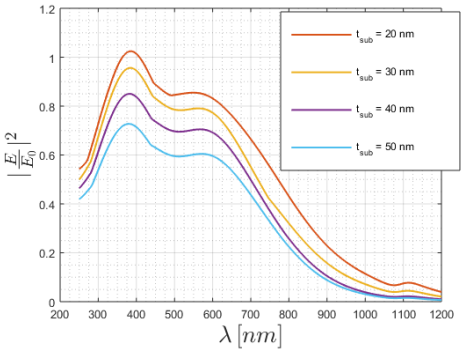

Fig. 10. Substrate thickness sweep on an aluminium nanostructure with a quartz substrate.

V. Sensors

Based on the appraisal done on the previous section, a structure is defined in order to develop a sensor. A sensor is a device which when exposed to physical or chemical phenomena - for example temperature, force, displacement, chemical elements concentration or chemical reaction -, produces a proportional output signal - for example optical, electrical, mechanical or thermal -, [33]–[35]. However, it is called a sensor because the sensor's input is an optical signal and its output is here only be studied as an optical signal too, due to the fact that the output is compared and referenced to the input. Nonetheless, several materials, such as the direct band-gap semiconductors, allow us to have an electrical output - voltage or current -, and so that, the device can be named as a transducer, thanks to its capability to generate a different output signal type in relation to the input one.

Based on the previous simulations, it is simulated a gold structure defined by a periodicity of $a_0 = 0.3\,\mu\text{m}$ and a hole diameter of $d = 120\,\text{nm}$ - which is 40% of the periodicity, as the relation between $a_0 = 0.5\mu\text{m}$ and $d = 200\,\text{nm}$ -. Moreover, the nanoantenna will have a thickness of $t = 50\,\text{nm}$ and the substrate a thickness of $t_{sub} = 20\,\text{nm}$. Priors tests were done in order to choose the substrate thickness. It is known that as the substrate thickness decreases, the maximum gain increases. However, on the previous tests the substrate described by $t_{sub} = 20\,\text{nm}$ presents a lower peak than for

$t_{sub} = 30\,\text{nm}$. Thus, the new nanostructure was tested for both combinations and it is going to be used the better one, which is $t_{sub} = 20\,\text{nm}$.

The result is shown on figure 11, where it is obvious that the result of a parameters combination creates a worst case in terms of gain when comparing with some of the previous simulated structures - for example when comparing with figure 9 -. Thus, it is possible to conclude that parameters results are not totally independent, and it was demonstrated when the hole diameter have to be scaled based on the periodicity relative percentage - in order not to create an impossible structure where the hole is bigger than its periodicity -. However, all the previous rules remain, *i.e.*, sweeping only one parameter having a reference structure will result the same as previous mentioned. The unpredictable problem occurs when more than one parameter is swept.

Nevertheless, the gold sensors will be characterised as reported before, which spectrum is illustrated on figure 11. It is reach a gain of 4.67 for $983\,\text{nm}$, having a gain region between $860\,\text{nm}$ and $1172\,\text{nm}$.

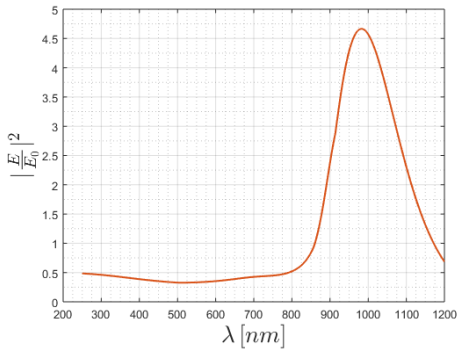

Fig. 11. Optical response of an air-gold-quartz nanostructure characterised by $a_0 = 0.3\,\mu\text{m}$, $d = 120\,\text{nm}$, $t = 50\,\text{nm}$ and $t_{sub} = 20\,\text{nm}$.

The sensor with the aluminium nanoantenna guarantees gain along all the visible region. The structure is the same of the sensor with gold. In order to create a flatter gain in the visible part of the spectrum two other values of the nanoantenna thickness were tested. However, these results were not satisfactory, and the initial structure was chosen. The corresponding simulation results are presented on figure 12. In this case, the final result is better than those resulting from independently varying the different parameters of the structure one by one.

A. General Purposes

A sensor is characterised by a parameter whose values change with the occurrence of something. The parameter change has to be measured. Nonetheless, simpler applications must be analysed first, in order not to break the reasoning, even that these applications are not defined as sensors. For this reason, some applications are going to be cover, using the lastly presented nanostructures and the responses. Depending

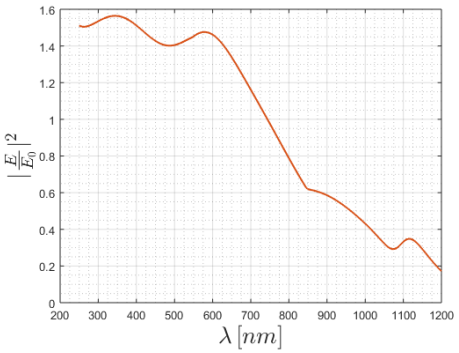

Fig. 12. Optical response of an air-aluminium-quartz nanostructure characterised by $a_0 = 0.3\,\mu\text{m}$, $d = 120\,\text{nm}$, $t = 50\,\text{nm}$ and $t_{sub} = 20\,\text{nm}$.

on the application the sensor can be optimised. The optimisation process depends on the different parts of the sensor, but in some situations the simple optimisation of the nanoantenna response to optimise the sensor.

An example is a nanoantenna of gold used to improve the sensibility of infrared sensors - for example on medical applications -, since some infrared wavelengths have high amplification and the others have huge attenuation. Then the output of sensor presents an improved sensitivity. Another example is the oximeter, where the sensor measures the amount of oxygen on blood. There are different types, from the portable to the hospital ones. In both cases, there are LED emitting two distinct signals, for example on the spectral red and blue regions. The optical spectrum of blood varies with the amount of oxygen, because cells can absorb more or less radiation according to the oxygen they transport. Thus, for example using the oximeter on fingers and analysing the output spectrum resulting from the photodetection of the red and blue light after the radiation propagates through cells, it is possible to determine the percentage of oxygen. In this case, nanoantennas can detect and amplify the detected radiation, in the two spectra interval of interest, replacing photodetectors and increasing the device sensibility. In this case, it is suggested that a gold nanoantenna can be used to detect the red signals and a silver one to detect the blues. The overall sensibility will increase, weak signals can be generated and detected, and small devices can be built.

The optical response of the nanostructure with a nanoantenna of gold can be used to improve LED and LASER - used for example in optical communications -, sensibilities in a certain wavelength band. As seen on the previous simulations, changing the material of the nanoantenna, it is possible to place the peak along the frequency/wavelength range. In the case of the spectrum on figure 11, a near-infrared region is amplified, specially around $1000\,\text{nm}$. Another example on communications applications is the use these nanoantennas to convert free-space energy into guided energy and *vice-versa*, as it is done by a regular antenna. In this case, in addition to this conversion, the structure can be tuned to filter and amplify, using just one miniaturised device.

Lastly, the aluminium nanostructure, whose spectrum is on

figure 12, can be used to amplify the visible and ultraviolet regions. An example of this application is on the concentration and amplification of the solar irradiance - which is predominant on the visible region -, incident on the active area of a solar cell, resulting in more incident power and consequently, on more generation of output power. However, it is necessary to guarantee the chemical stability of aluminium for long-term applications.

B. Temperature Sensor

The first sensor - in the strict sense of the definition - , is the temperature one, *i.e.*, a thermometer. To simulate this sensor, it is necessary to have experimental results or models for the dependence of the optical properties with the temperature. However, it is very difficult to find available results on literature.

It was impossible to find air and quartz models for different temperatures. However, as these materials do not have interband region on the simulated range, it is not necessary to have its models. On the other hand, the temperature has small influence on the dielectric function real part, in comparison with the imaginary one. Thus, the influence of the metal will always be the predominant and so that, structures as the ones presented in this work can be used as temperature sensors [19]–[21].

A temperature sensor based on a gold nanoantenna is going to be simulated, for five different temperatures, T, - 23 °C, 100 °C, 200 °C, 250 °C and 300 °C -, using models for each temperature [38]. The real part of the gold dielectric function is almost independent of the temperature until approximately a wavelength of 550 nm [38]. After it, the temperature dependence can be divided into two different groups. First, for each wavelength, as the temperature increase, the real part of the dielectric function becomes smaller [38]. However, there is a specific temperature value - the critical temperature value(s) -, where an inversion of this rule starts. In this case, between $T = 200\,°\mathrm{C}$ and $T = 250\,°\mathrm{C}$, there is a value of what the real part of the dielectric function becomes abruptly higher than the values for smaller temperatures [38]. After that, as higher the temperature is, the higher the real part of the dielectric function will be [38]. On the other hand, the imaginary part seems to have a temperature dependency along all the simulated range however, only above approximately a wavelength of 600 nm a strict rule seems to be established [38]. Below it, the dependency is not well defined. Howsoever, the model analysis is not the most important, because the output optical response have yet to be verified, and is this spectral response that will allow to conclude about the sensor designing.

In this case, and for this range of temperatures, there is only one of these temperature values - known as critical temperature -, which is between $T = 200\,°\mathrm{C}$ and $T = 250\,°\mathrm{C}$. Thus, it is possible to study this sensor in two different work regions: the first where the peak value increases with the temperature and the second where this value decreases as the temperature increases. On figures 13 and 14 are respectively illustrated the nanostructure behaviour, both for temperatures below the critical one and for temperatures above the critical one.

There, it is observable that is possible to differentiate each temperature only using the maximum gain value. Moreover, as expected, the conclusions taken from the complex dielectric function analysis is reflected on the nanostrucutre response.

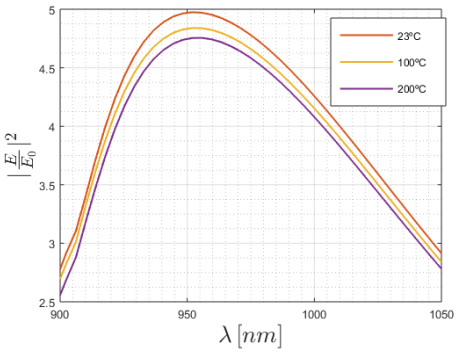

Fig. 13. Gold nanostructure response for different temperatures, for temperatures below the critical one.

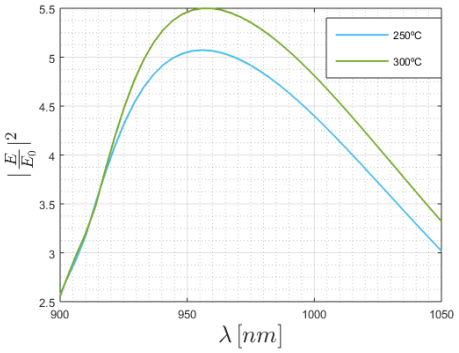

Fig. 14. Gold nanostructure response for different temperatures, for temperatures above the critical one.

Furthermore, based on figure 15, which is the combination of the responses shown of figures 13 and 14, it is quite impressive how the spectrum remains the same shape and intensity values, in spite of the temperature variation, excepting on the work region - the peak values -.

These simulations allow us to conclude that each temperature will generate a different nanostructure response, which is well defined. Thus, measuring the output spectrum at wavelengths near the peak one, it is possible to determine what is the temperature around the nanostructure, since different temperatures produce different output electric field norms.

Other conclusion is that it is possible to know the temperature measuring a single wavelength, if known the critical temperature values and without the necessity of go through all the range. If the peak value - and a uncertainty range - , is specify for each structure, it is possible to use only one wavelength measurements, since around the peak there are not equal values for different temperature.

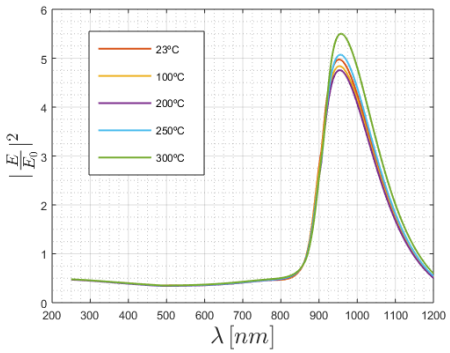

Fig. 15. Gold nanostructure response for different temperatures.

Even more, based on previous results, it may appear that these sensors are not able to detect small temperature variations - it seems that they have small sensibilities -. However, they can be used to detect temperature ranges, for example, to analyse the occurrence of certain chemical reactions.

Finally, the last conclusion that have to be clearly explicit is the possibility of produce electrical energy. First, at around the room temperature the nanostructure has already optical gain however, after a certain temperature, the gain will increase as the temperature increase. For that reason, it is possible to tune the energy production and actually generate energy using, for example, chemical reactions to produce heat and the environment radiation - which is the opposite of having the nanoantenna as temperature sensor for chemical reactions-.

C. Tissues Detection Sensor

The possibility to detect different tissues, using their optical properties and these nanoantennas was tested. Four models were found for this wavelength range - liver tissues, colon mucosa tissues, colon submucosa tissues and colon serosa tissues -, and the main goal is to use the gold and the aluminium nanostructures in order to detect the tissue over the nanoantenna [32]. As illustrated on figure 16, the structure is going to be based on the one described before. However, the tissues are placed between the dielectric and the nanoantenna. Thus, the nanoantenna holes will be covered by those tissues instead of the dielectric. The tissue medium has a thickness of $200\,\mathrm{nm}$, but only $150\,\mathrm{nm}$ are visible on the figure, since the remaining is the nanoantenna thickness. The dielectric has also a thickness of $150\,\mathrm{nm}$.

Due to the models wavelength range, the following simulations were done between $450\,\mathrm{nm}$ and $1200\,\mathrm{nm}$.

First, the gold made nanostructure is simulated considering the aforementioned tissues and its results are presented on figure 17, where it is possible to verify that all the tissues responses are similar. It is noticeable that different tissues will produce different spectral peaks. In this case, it is possible to distinguish liver and three types of colon tissues. As expected, the difference among colon tissues is smaller than the difference between any colon tissue and the liver one.

However, analysing the spectral region near the peak, it is possible to better observe that even the colon tissues can

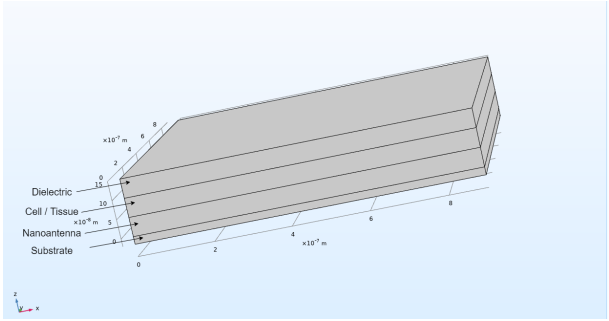

Fig. 16. Topology of the simulated sensor structure.

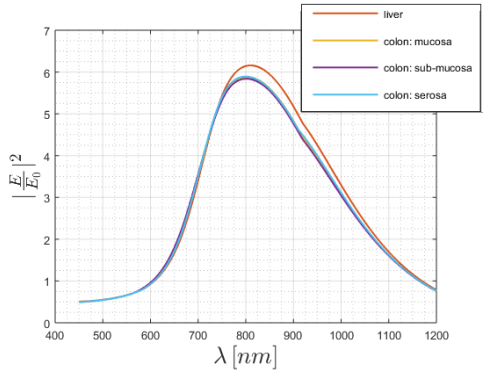

Fig. 17. Gold nanostructure response for different human body tissues.

be differentiate among them, as illustrated on figure 18, in different wavelengths.

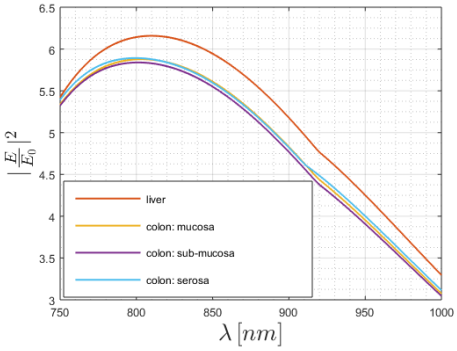

Fig. 18. Gold nanostructure response for different human body tissues (zoom).

The same simulations were done using the aluminium nanoantenna, which results are presented on figure 19. There, although all the responses are very similar at higher wavelengths, the region around $500\,\mathrm{nm}$, that is in focus on figure 20, allows the detection of each tissue. Once again, the liver can be easily differentiate from the colon cells however, it can be possible to distinguish similar tissues, as the colon ones.

One way of distinguish more similar characteristics is to do this analysis along all the spectrum, because there are more than one single region where the tissues lead to different responses values. Nonetheless, based on which are the tissues to distinguish, it can be possible to use just one single

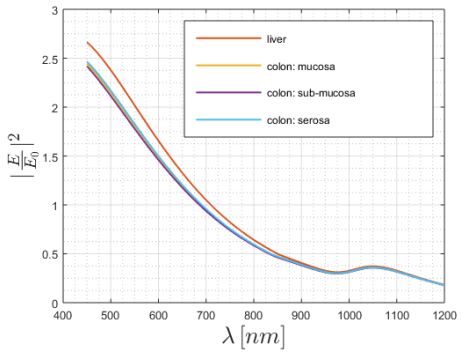

Fig. 19. Aluminium nanostructure response for different human body tissues.

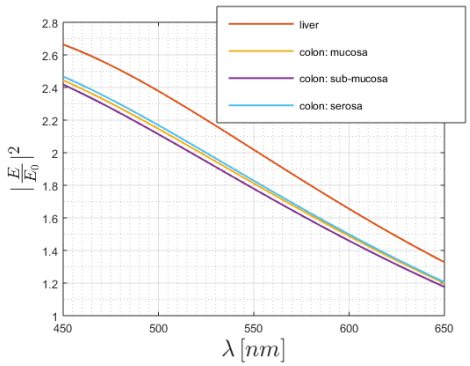

Fig. 20. Aluminium nanostructure response for different human body tissues (zoom).

wavelength. For example, to distinguish liver from one of the colon samples, it is possible to use just one wavelength however, to distinguish similar tissues, as the colon ones, it is much better to analyse all the range. Furthermore, to increase the accuracy of this method, it can be used several different structures - different materials, parameters and typologies -, in order to have different responses to compare and increase the method reliability.

In addition, it can be possible to create a huge database of optical responses like these for each tissue. Some of them should be unhealthy tissues, for example cancer cells at different stages or cells affected by diseases as diabetes [39]. Thus, there are already some studies that report the variation of the optical properties with some diseases [39]. Then, the spectral response will vary and it is possible to monitor cells and tissues in real time, *in vitro* or *in vivo*, in order to create a regular report of spectra like these [8], [22], [23], [25]. It is useful to detect some diseases or to control substances levels [8], [19], [22]–[24], [36], [37]. For instance, if optical properties vary with the concentration of some substance, it is possible to take conclusions regarding the spectral analysis. It is the case of insulin levels - diabetes -, or, the blood pressure or oxygen in circulation. Nonetheless, it is very important to have a huge database, in order to create a complex dielectric function model to use on these applications. These real models are not easily available.

VI. Conclusion

The discovery of the extraordinary optical transmission questioned all the classical theories of diffraction of the electromagnetic field. None of them explain the new phenomenology, because it is assumed the existence of ideal materials, namely metals. In doing so the generation and propagation of surface plasmon polaritons and of creeping waves is not considered and, consequently, the classical theories fail. The consideration of these effects demands the consideration of the electrical and optical properties of real materials, through a correct modelling of the dielectric function and refractive index. Then the propagation of surface plasmons polaritons can be theoretically analysed from Maxwell's equations. Their generation and propagation, combined with the propagation of creeping waves – specially out of the visible spectral region -, allow to describe the extraordinary optical transmission phenomenon. This phenomenon can be observed using nanoantennas. This kind of structures allow the concentration and amplification of electromagnetic energy.

Using *COMSOL Multiphysics* it was created a 3D simulation environment to model and simulate a nanoantenna, obtaining its optical response. The optical response is dependent on the used materials, on the nanoantenna and also in the surrounding materials.

Furthermore, it is possible to verify that for the gold nanostructure, as the structure periodicity increases, the maximum intensity value decreases, keeping the same peak wavelength value. On the aluminium spectra, it is concluded the periodicity affects the flatter region, the region that can have gain. In relation to the hole diameter sweep, it is possible to verify that as larger the hole is, the higher the intensity peak is. However, in this case, a careful conclusion should be taken, because it is also known that the hole diameter should be much smaller than the incident wavelength. In addition to this effect, red-shifts will occur as the diameter increases. The nanoantenna thickness is also analysed. Considering the previous simulations, it is possible to conclude that as thicker the nanoantenna is, the less the peak intensity will be. Also, blue-shifts will occur in this situation and, specifically on the aluminium response, it seems that the flat region becomes flatter. The substrate thickness leads to the idea of adjusting losses and consequently gains without changing the spectrum shape. The thicker the substrate is, the higher the losses are, keeping the optical response shape.

The simulations' results also lead to conclude that the spectral response can be tuned by varying the topology and the parameters of the structure. However, in order to create rigorous analytical models, a huge simulation database have to be created, requiring huge computational efforts. Furthermore, all the simulations show high amplification and concentration of the electromagnetic field near the interfaces. This is a clear evidence of the generation and propagation of surface plasmon polaritons.

The nanostructure of gold was simulated as a temperature sensor, using models for the complex dielectric function in-

cluding the temperature. A nanostructure like this can behave as a temperature sensor with a critical temperature. Below this critical value the peak of the optical response decreases with the increase of temperature, but the corresponding wavelength remains almost constant. Above the critical value, the peak of the optical response increases with temperature and the peak wavelength is slightly shifted to a greater wavelength.

A sensor to distinguish human body tissues was also simulated using the gold and the aluminium nanostructure. The simulated structures can distinguish different tissues and even detect diseases. However, to detect diseases, it is very important to have a huge database in order to create models of the electrical permittivity – complex dielectric function -, of healthy and unhealthy tissues. The creation of good models for the different structures, and the creation of new structures, used to distinguish the human tissues and detect the diseases, is also very important.

To sum it up, some structures based on the occurrence of extraordinary optical transmission, were modelled and simulated. Several simulations were presented to discuss the influence of the materials and of the geometrical parameters on the optical response of the structures. The obtained results clearly point to the development of the project of miniaturised sensors, that could be used to detect and measure temperature variations, to distinguish different human tissues and, consequently, in some cases to detect diseases.

REFERENCES

[1] Deus, J.D., et al. Princípio de Huygens. *Introdução à Física*; Escolar Editora: Lisboa, Portugal, 2014; pp. 68-88.

[2] Hecht, E. *Óptica*; Fundação Calouste Gulbenkian: Lisboa, Portugal, 2012; pp. 495-578.

[3] Ebbesen, T. W., et al. Extraordinary optical transmission through sub-wavelength hole arrays. *Nature* **1998**, *391*, 667.

[4] Gomes, R.D.F.R., Martins, M.J., Baptista, A. et al. Study of an Optical Antenna for Intersatellite Communications. *Opt Quant Electron* **2017**, *49*, 135.

[5] Sharma, N., et al. Fuchs Sondheimer–Drude Lorentz model and Drude model in the study of SPR based optical sensors: A theoretical study. *Optics Communications* **2015**, *357*, 120-126.

[6] Barchiesi, D. and Grosges, T. Fitting the optical constants of gold, silver, chromium, titanium, and aluminum in the visible bandwidth. *Journal of Nanophotonics*, **2014** *8.1*, 083097.

[7] Gu, Y., et al. Color generation via subwavelength plasmonic nanostructures. *Nanoscale* **2015**, *7.15*, 6409-6419.

[8] Ji, J., et al. High-Throughput Nanohole Array Based System To Monitor Multiple Binding Events in Real Time. *Analytical Chemistry* **2008**, *80(7)*, 2491-2498.

[9] Wissert, M. D., et al. Nanoengineering and characterization of gold dipole nanoantennas with enhanced integrated scattering properties. *Nanotechnology* **2009**, *20.42*, 425203.

[10] Li, J.Y., et al. Influence of hole geometry and lattice constant on extraordinary optical transmission through subwavelength hole arrays in metal films. *Journal of Applied Physics* **2010**, *107.7*, 073101.

[11] Biagioni, P., et al. Nanoantennas for visible and infrared radiation. *Reports on Progress in Physics* **2012**, *75*, 024402.

[12] Mohammadi, A., Sandoghdar, V., and Agio, M. Gold, copper, silver and aluminum nanoantennas to enhance spontaneous emission. *Journal of Computational and Theoretical Nanoscience* **2009**, *6.9*, 2024-2030.

[13] Novotny, L. and Niek, V. H. Antennas for light. *Nature photonics* **2011**, *5.2*, 83.

[14] Wu, S., et al. Dielectric thickness detection sensor based on metallic nanohole arrays. *The Journal of Physical Chemistry C* **2011**, *115.31*, 15205-15209.

[15] Tsiatmas, A. et al. Superconducting plasmonics and extraordinary transmission. *Applied Physics Letters* **2010**, *97.11*, 111106.

[16] Brolo, A.G., et al. Surface Plasmon Sensor Based on the Enhanced Light Transmission Through Arrays of Nanoholes in Gold Films. *Langmuir* **2004**, *20(12)*, 4813-4815.

[17] Gordon, R. Extraordinary optical transmission for surface-plasmon-resonance-based sensing. *Nanophotonics* **2008**, *2*, 206.

[18] Gordon, R., et al. A new generation of sensors based on extraordinary optical transmission. *Accounts of chemical research* **2008**, *41.8*, 1049-1057.

[19] Unser, S., et al. Localized surface plasmon resonance biosensing: current challenges and approaches. *Sensors* **2015**, *15.7*, 15684-15716.

[20] Sen, M. A. Design and development of calorimetric biosensors using extraordinary optical transmission through nanohole arrays. **2012**.

[21] Kowalski, G.J., et al. Fast Temperature Sensing Using Changes in Extraordinary Transmission Through an Array of Subwavelength Apertures. *Optical Engineering* **2009**, *48.10*, 104402.

[22] Yang, J.C., et al. Metallic Nanohole Arrays on Fluoropolymer Substrates as Small Label-Free Real-Time Bioprobes. *Nano Letters* **2008**, *8(9)*, 2718-2724.

[23] Hill, R. T. Plasmonic biosensors. *Wiley Interdisciplinary Reviews: Nanomedicine and Nanobiotechnology* **2015**, *7.2*, 152-168.

[24] Etezadi, D., et al. Nanoplasmonic mid-infrared biosensor for in vitro protein secondary structure detection. *Light: Science & Applications* **2017** *6.8*, e17029.

[25] Sangwan, A., et al. Increasing the Communication Distance Between Nano-Biosensing Implants and Wearable Devices. *2018 IEEE 19th International Workshop on Signal Processing Advances in Wireless Communications (SPAWC)*, **2018**.

[26] Bethe, H. A. Theory of diffraction by small holes. *JPhysical review* **1944**, *66.7-8*, 163.

[27] Bouwkamp, C. J. On Bethe's Theory of Diffraction by Small Holes. *Philips Research Reports* **1950**, *5*, 321-332.

[28] Ritchie, R. H. Plasma losses by fast electrons in thin films. *Physical review* **1957**, *106.5*, 874.

[29] Ritchie, R. H., et al. Surface-plasmon resonance effect in grating diffraction. *Physical Review Letters* **1968**, *21.22*, 1530.

[30] Raether, H. Surface plasmons on smooth surfaces. In *Surface plasmons on smooth and rough surfaces and on gratings.*; Springer: Heidelberg, Berlin, Germany, 1988; pp. 4-39.

[31] Lalanne, Ph., Hugonin, J. P. Interaction between optical nano-objects at metallo-dielectric interfaces. *Nature Physics* **2006**, *2.8*, 551.

[32] Refractive index database - refractive index. Available online: https://refractiveindex.info/ (last access on 17 April 2020).

[33] Yurish, S. Y., and Gomes, M. T. (editors). *Smart Sensors and MEMS: Proceedings of the NATO Adavanced Study Institute on Smart Sensors and MEMS Portugal 8-19 September 2003*; Springer Science & Business Media: Povoa de Varzim, 2005: Vol. 181.

[34] Kirianaki, N. V., Yurish, S. Y., Shpak, N. O., and Deynega, V. P. *Data acquisition and signal processing for smart sensors*; Wiley: Chichester, England, 2002; pp. 72-78.

[35] Webster, J. G. and Fox, S. (editors), *Measurement, Instrumentation and Sensors Handbook*, Springer Science & Business Media, 1999.

[36] Rakhshani, M. R., and Mansouri-Birjandi, M. A. High sensitivity plasmonic refractive index sensing and its application for human blood group identification. *Sensors and Actuators B: Chemical* **2017**, *249*, 168-176.

[37] Wolf, M., Gulich, R., Lunkenheimer, P., and Loidl, A. Broadband dielectric spectroscopy on human blood. *Biochimica et Biophysica Acta (BBA)-General Subjects* **2011**, *1810(8)*, 727-740.

[38] Reddy, H., Guler, U., Kildishev, A. V., Boltasseva, A., and Shalaev, V. M. Temperature-dependent optical properties of gold thin films. *Optical Materials Express* **2016**, *6(9)*, 2776-2802.

[39] Grigorev, R., Kuzikova, A., Demchenko, P., Senyuk, A., Svechkova, A., Khamid, A., and Khodzitskiy, M. Investigation of Fresh Gastric Normal and Cancer Tissues Using Terahertz Time-Domain Spectroscopy. *Materials* **2020**, *13(1)*, 85.